Essay

X-ray Tomography Generates 3-D Reconstructions of the Yeast, *Saccharomyces cerevisiae*, at 60-nm Resolution

Carolyn A. Larabell*†‡ and Mark A. Le Gros†

*Department of Anatomy, University of California, San Francisco California 94143; and †Life Sciences Division, Lawrence Berkeley National Laboratory, Berkeley, California 94720

We examined the yeast, *Saccharomyces cerevisiae*, using X-ray tomography and demonstrate unique views of the internal structural organization of these cells at 60-nm resolution. Cryo X-ray tomography is a new imaging technique that generates three-dimensional (3-D) information of whole cells. In the energy range of X-rays used to examine cells, organic material absorbs approximately an order of magnitude more strongly than water. This produces a quantifiable natural contrast in fully hydrated cells and eliminates the need for chemical fixatives or contrast enhancement reagents to visualize cellular structures. Because proteins can be localized in the X-ray microscope using immunogold labeling protocols (Meyer-Ilse *et al.*, 2001. J. Microsc. *201,* 395–403), tomography enables 3-D molecular localization. The time required to collect the data for each cell shown here was <15 min and has recently been reduced to 3 min, making it possible to examine numerous yeast and to collect statistically significant high-resolution data. In this video essay, we show examples of 3-D tomographic reconstructions of whole yeast and demonstrate the power of this technology to obtain quantifiable information from whole, hydrated cells.

INTRODUCTION

The budding yeast, *Saccharomyces cerevisiae*, has long been a valuable model system for genetic, molecular, and biochemical analyses and continues to be important for modern proteomics investigations. Most recently large-scale efforts have been made to characterize protein complexes using mass spectrometry and tandem-affinity purification (TAP; Gavin *et al.,* 2002; Ho *et al.,* 2002). As a result, hundreds of distinct multiprotein complexes have been identified and new cellular roles for several hundred other proteins, most of which had no previous functional annotation, have been proposed. An important method for gaining insight into the function of a protein is to determine its location in cells. Kumar *et al.* (2002) recently conducted a high throughput immunofluorescent localization of tagged gene products in the budding yeast and determined the subcellular location of 2744 proteins. By extrapolating these data through a computational algorithm that uses a Bayesian estimation system, they concluded that the entire yeast proteome encompasses ~5100 soluble proteins and more than 1000 transmembrane proteins, 47% of which are cytoplasmic, 13% mitochondrial, 13% exocytic (including proteins labeling endoplasmic reticulum and secretory vesicles), and 27% nuclear/nucleolar. This is a remarkable undertaking that begins to provide insight into protein locations and their associated function. However, if the yeast proteome encompasses 30,000 protein interactions, many of which change during the organism's life cycle (Kumar and Snyder, 2002), more precise information about the location of each protein throughout the cell cycle will be required. This information is beyond the level of resolution of existing light microscopy techniques and is unattainable using electron microscopy, given the time-consuming nature of the requisite specimen preparation. New high-throughput, high-resolution imaging techniques are imperative for such extensive investigations. We show here that X-ray tomography, an emerging technique for imaging cells, has the potential to accomplish these goals and make significant contributions to our understanding of protein function in cells.

Soft X-ray microscopy combines features associated with both light and electron microscopy. It is fast and relatively easy to accomplish (like light microscopy), and it produces high-resolution, absorption-based images (like electron microscopy). As with light microscopy, one can examine whole, hydrated cells. In the energy range of the photons used (between the K shell absorption edges of carbon [284 eV, $\lambda = 4.4$ nm] and oxygen [543 eV, $\lambda = 2.3$ nm]), organic material absorbs approximately an order of magnitude more strongly than water, producing a quantifiable natural contrast and eliminating the need for contrast enhancement procedures to visualize cellular structures (Weiss *et al.,* 2000; Schneider *et al.,* 2002). Using this approach, superb structural information can be obtained from whole, hydrated cells at better than 35-nm resolution. In addition, molecules can be localized using protocols that combine the ease of immunfluorescence labeling with the higher-resolution capabilities of X-ray imaging (Meyer-Ilse *et al.,* 2001). These capabilities, combined with tomographic procedures, offer unique three-dimensional (3-D) views of cells.

Tomography is a familiar tool for obtaining 3-D information in diagnostic medical imaging. Similar technology is being used today to generate remarkable 3-D views of select specimens, including microorganisms, thin regions (<0.5 μm) of crawling cells, and sections of cells, using electron
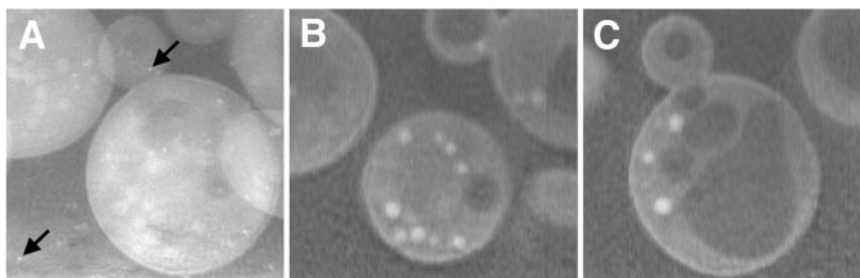
Figure 1. X-ray images of the budding yeast, *Saccharomyces cerevisiae*. (A) Projection image of yeast in the capillary; arrows indicate 60-nm gold balls used as fiducial markers for alignment of all images for tomographic reconstruction. (B and C) Computer-generated sections from the reconstructed data; X-ray dense lipid droplets (small white circles) are now easily distinguished as distinct organelles and large vacuoles that are less dense appear dark. Yeast cell, 5 μm diameter.

microscopy (Grimm *et al.,* 1998; Baumeister *et al.,* 1999; O'Toole *et al.,* 1999; Martone *et al.,* 2000; Nicastro *et al.,* 2000; Marsh *et al.,* 2001; Fernandez *et al.,* 2002; Medalia *et al.,* 2002). This approach reveals extraordinary details, but it is too tedious and time-consuming for high-throughput analyses. X-ray tomography is quite straightforward and rapidly generates 3-D, quantifiable information from whole cells. This technique was recently used to examine rapidly frozen algae (Weiss *et al.,* 2000) and fixed *Drosophila* cells (Schneider *et al.,* 2002).

We show here that tomographic reconstructions of rapidly frozen yeast, *S. cerevisiae,* produce remarkable 3-D views of these small cells at ~60-nm resolution. Recent automation of data collection, which enables collection of images at 1° intervals in 3 min, assures that future reconstructions will approach 35-nm resolution. Using this technology, it is now possible to rapidly examine phenotypic consequences of genetic mutations and knockouts and observe changes not detectable with light microscopy. It is also possible to obtain quantifiable, 3-D information about the localization of molecules throughout the entire cell. X-ray tomography is the first high-throughput, suboptical resolution imaging technology.

MATERIALS AND METHODS

Preparation of Cells and Freezing

Yeast, *S. cerevisiae,* were grown with rotary shaking at 25°C in liquid YPD medium (1% yeast extract, 2% bapto peptone, 2% glucose). Just before imaging, they were loaded into a 10-μm-diameter capillary from the beveled tip end of the capillary using an Eppendorf microinjection apparatus (Eppendorf InjectMan Nl2 Manipulation System; Brinkmann Instruments, Westbury, NY). The yeast were examined in the light microscope then rapidly frozen with a blast of liquid-nitrogen–cooled Helium gas, placed in the X-ray microscope, and maintained at cryogenic temperatures throughout data collection as described previously (Meyer-Ilse *et al.,* 2001).

Microscopy and Tomographic Reconstruction

The images were collected using a transmission X-ray microscope with photon energies just below the oxygen edge, i.e., 517 eV (corresponding to a wavelength of λ = 2.4 nm). Images were formed using a Fresnel zone plate for the condenser and objective lens. The condenser lens is 9 mm in diameter with an outermost zone width of 55 nm and a focal length of 205 mm at 517 eV

photon energy (2.4 nm). The objective zone plate lenses are 45 μm in diameter, have an outermost zone width of 35 nm, and a focal length of 650 μm at 517 eV photon energy. The spatial resolution is largely determined by the width of the outermost zone of the objective zone plate and, as described previously, is on the order of 35–40 nm when examining cells grown on silicon nitride windows (Meyer-Ilse *et al.,* 2001). For tomography, 45 images were collected at 4° intervals through 180° of rotation. The projection series was then aligned to a common axis of rotation and a 3-D volume reconstruction was performed using weighted, filtered back projection (Frank *et al.,* 1996). The magnified image was recorded on a Peltier-cooled, back-illuminated, 1024 × 1024 soft X-ray CCD camera (Roper Scientific Instruments Micromax system with SIT chip; Roper Industries, Inc., Duluth, GA).

Volume Visualization

Surface reconstruction and volume segmentation and rendering were performed using AmiraDev 3 software (TGS, Inc., San Diego, CA), incorporating fast volume-rendering hardware, Volpro 500 (www.terarecon.com).

RESULTS AND DISCUSSION

Tomography is a powerful way to retrieve 3-D information from thick specimens. Because this requires collection of multiple projection images over a wide range of projection angles, cryo-fixed specimens are typically used for X-ray tomography. All cells shown here were live just before being placed in the glass capillary and rapidly frozen; because they had not been exposed to any chemical fixatives or contrast enhancement reagents, they closely resemble the native state. Collection of each data set is extremely simple and straightforward. Because each capillary contains rows of aligned yeast, it is possible to collect multiple tomographic data sets by simply advancing the capillary into the field of view. The capillary sample geometry also makes it possible to collect images from a 360° range of angles as it is rotated around an axis perpendicular to the X-ray beam. This eliminates the loss of data that occurs due to obstruction by the flat specimen holders that can only be rotated ±70°. Because of the cylindrical sample configuration, there is no missing wedge of spatial frequency information that typically occurs with electron tomography of cell sections.

The yeast were maintained at cryogenic temperatures with liquid-nitrogen–cooled helium gas during data collection (Meyer-Ilse *et al.,* 2001). Forty-five full-field projection
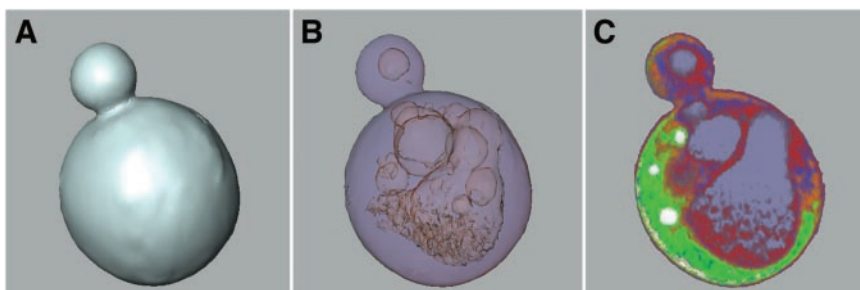

Figure 2. Reconstructed data of the yeast shown in Figure 1 using different volume analysis algorithms. (A) Opaque surface extraction; (B) transparent surface analysis showing internal vesicles; (C) volume rendered thick-slice section with different colors indicating degree of X-ray absorption; dense lipid droplets are white, less dense vacuoles appear gray, structures of varying densities appear green, orange, and red. Yeast cell, 5 μm diameter.

Figure 3. Cryo X-ray tomography of whole yeast, *S. cerevisiae*, viewed using several processing algorithms after reconstruction. (A) Combination of translucent outer surface and opaque surfaces that demark internal organelles; arrow points to nucleus that has been color-coded blue; (B) surfaces from A combined with volume rendering; arrow points to nucleus that is colored blue, lipid droplets appear white, and the surface of a large vacuole in the center of the yeast is color-coded pink; (C) 0.5-μm-thick section that had been volume-rendered according to the amount of X-ray absorption; lipid droplets are white, the internal structures of the vacuole and nucleus (arrow) appear red, and other cytoplasmic structures appear green and orange. Yeast cell, 5 μm diameter.
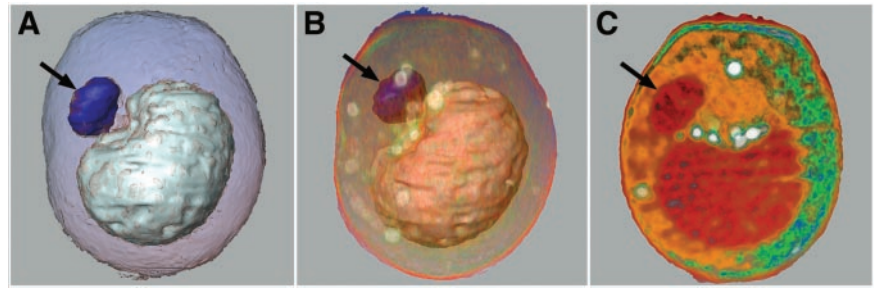
images were collected at 4° intervals through 180° degrees of rotation for each reconstruction. All 45 images were then aligned to a common axis of rotation using 60-nm-diameter gold particles as fiducial markers (arrows, Figure 1) and a fiducial marker alignment routine which is part of the "SPIDER" software suite of programs (Frank *et al.,* 1996). A single projection image of a typical field of view showing one budding yeast and portions of several nearby yeast is shown in Figure 1A. Although it is possible to see numerous overlapping vesicles and organelles inside of the yeast (Figure 1A, small white circles), it is difficult to distinguish the precise boundaries of these organelles because this image is a superimposition of all structures located in the 5-μm-thick yeast. The simplest way for the eye to interpret the 3-D nature of the raw data is to animate the entire series of 45 projection images, which immediately provides depth to the data set (Video Sequence 1).

Although the yeast appears more 3-D in the animation, it is still difficult to distinguish distinct organelle boundaries in any one of the projection images because of the degree of overlapping information. Tomographic reconstruction retrieves the 3-D information and reveals the internal structures of the cell. Two of the 110 computer-generated sections through the yeast, each of which is ~30 nm thick, are shown in Figure 1, B and C, and all 110 sections, slicing longitudinally through the capillary, can be played back as a video (Video Sequence 2). Several centrally located large vacuoles are clearly seen along with numerous smaller organelles around the periphery of the cell. These cortical organelles

are most likely endoplasmic reticulum and mitochondria, based on their position and previous data obtained from electron micrographs, but specific labeling is being conducted to definitively identify these structures as seen in X-ray tomography.

The X-ray microscope images were collected at X-ray energies of 514 eV, which lies within what is referred to as the "water window" wavelength range where organic material absorbs approximately an order of magnitude more than water. This produces a quantifiable natural contrast of biological material and eliminates the need for contrast enhancement procedures to visualize cellular structures of the yeast. Once a 3-D map of the X-ray absorption coefficient has been obtained, volume processing and visualization techniques can be used to analyze the data. One such visualization algorithm was used to extract the surface of the same yeast (Figure 2A and Video Sequence 3), whereas edge enhancement algorithms reveal numerous internal organelles of varying sizes (Figure 2B). The surfaces of organelles are seen in each of the individual images which, when played back as a movie, assume a very 3-D nature and illustrate the overall structural organization of the entire yeast (Video Sequence 4).

Because we are using absorbance contrast X-ray microscopy, we can color-code the cellular structures based on their density as determined by the volume-reconstructed X-ray absorption coefficient (Figure 2C). The lipid droplets, which are the densest structures, were color-coded white, the least dense vacuoles were color-coded gray, and numer-
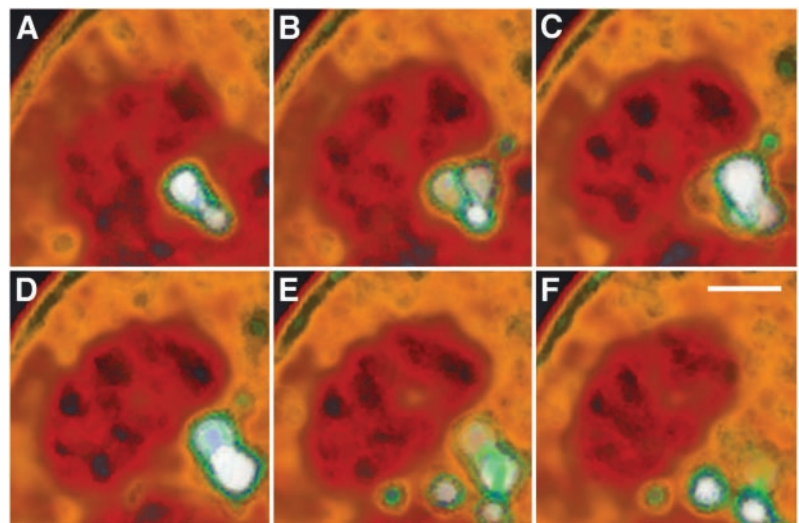

Figure 4. Computer-generated sections through the nucleus of the yeast seen in Figure 3. Six sections through the nucleus show internal organization of the nucleoplasm; dense lipid vesicles (white structures) are also seen adjacent to the nucleus. Bar, 0.5 μm.
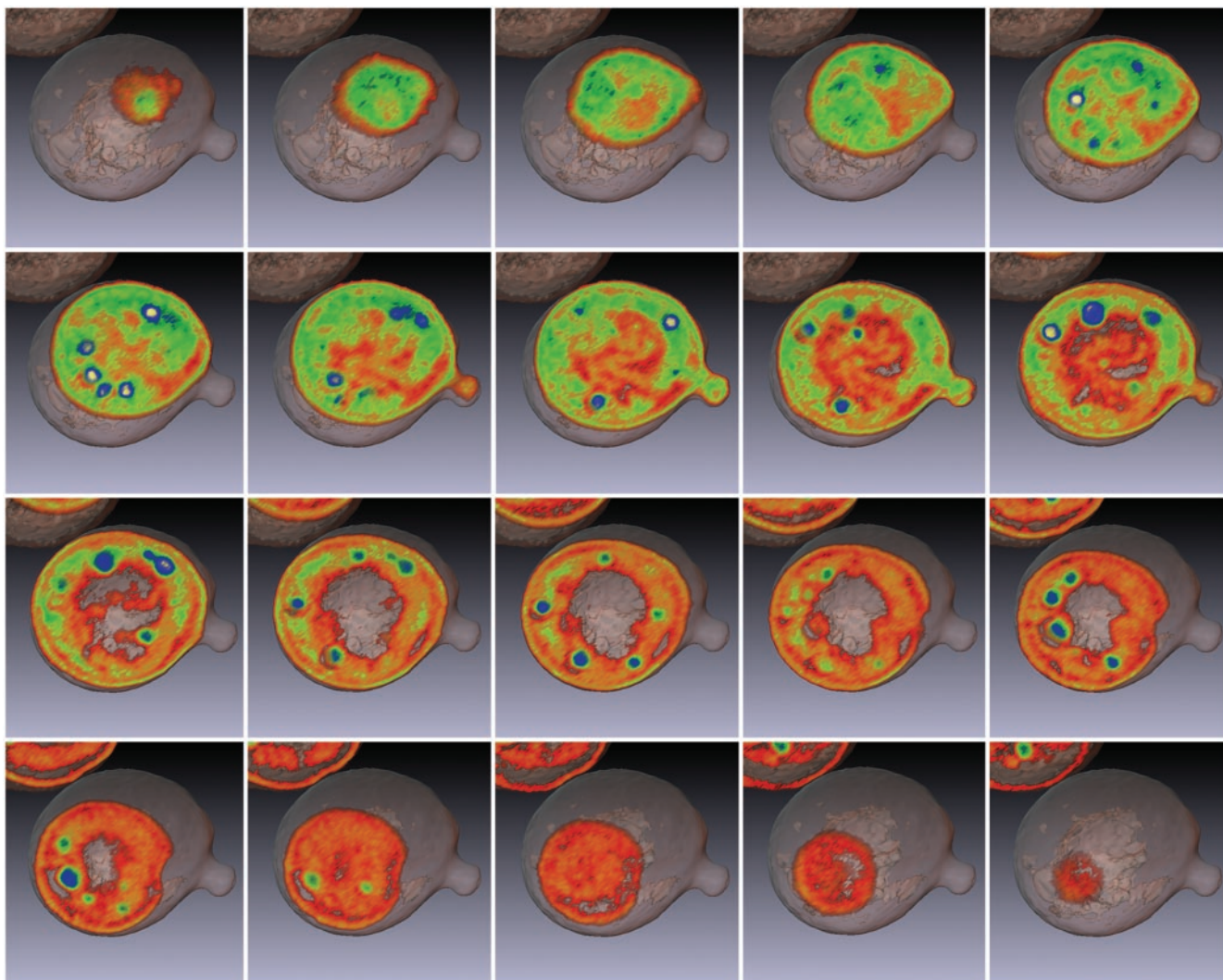
Figure 5. Computer-generated sections through the tomographic reconstruction of an early budding yeast. Structures have been assigned different colors, which indicate degree of X-ray absorption. Dense lipid droplets appear white and other cell structures are colored shades of blue, green, and orange with decreasing density. Yeast cell, 5 μm diameter.

ous other subcellular structures of intermediate densities were colored shades of green, orange, and red. To see all structures throughout the yeast, the entire stack of 110 computer-generated sections are played as a movie (Video Sequence 5). When these volume-rendered sections are superimposed on the transparent surfaces that were shown in Figure 2B and the data are played back as a movie (Video Sequence 6), the quantifiable absorption-based data are seen superimposed on the 3-D structural information in the yeast.

We also examined nondividing yeast and collected complete tomographic data sets as described for Figures 1–3. After alignment of the raw data and tomographic reconstruction, various visualization algorithms were applied to reveal the internal structures of the yeast (Figure 3). One such algorithm, which renders the cell surface transparent, reveals prominent internal organelles that have been colorcoded based on their density. The cell nucleus, which has been color-coded dark blue, is located immediately adjacent to a large vacuole, which has been color-coded cyan (Figure 3A and Video Sequence 7). By using a combination of the X-ray absorption coefficient segmentation and 3-D volume

rendering using a ray cast algorithm, multiple additional internal vesicles are revealed, including the extremely dense lipid droplets (white circles, Figure 3B). When the complete data set is played back as a video, unique 3-D views of the structural organization of the yeast components emerge (Video Sequence 8). These organelles were further examined by color-coding them according to the calculated X-ray absorption coefficient, as was described for Figure 2C. Now, as shown in one of the sections from this data set (Figure 3C), the organelles are seen in computer-generated cross sections, each of which is ~30 nm thick. These same data can be played back as a video, showing all 150 sections (Video Sequence 9) or as an animation of thick cut-away sections positioned perpendicularly to each other (Video Sequence 10). Additional details of the nuclear structure can be seen at higher magnification in six computer-generated sections through this region of the cell (Figure 4). Another algorithm was used to reveal the internal structures of a yeast cell in the very early stages of budding as shown in a series of computer-generated sections through the reconstructed data (Figure 5). These structures were color-coded based on the
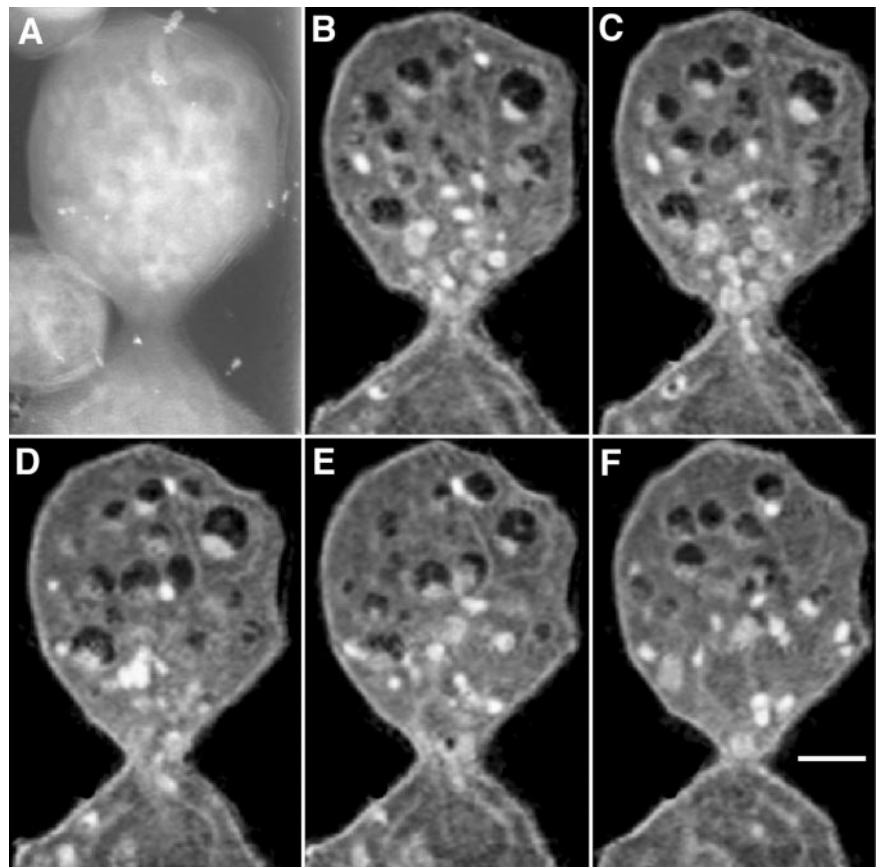
Figure 6. High-magnification view of a budding yeast. (A) Projection image showing numerous superimposed organelles. (B–F) Computer generated sections through the yeast reveals numerous organelles after tomographic reconstruction; the most dense (bright white circles) are filled with lipid. Bar, 0.5 μm.

X-ray absorption coefficient, highlighting numerous organelles and vacuoles. Every tenth computer section through the yeast is shown here, and all of the sections can be played back as a video (Video Sequence 11).

The ability to retrieve structural information using X-ray tomography techniques is best demonstrated in high-magnification views of the bud neck region (Figure 6). A single projection image (Figure 6A) shows the lack of discernible structural information in the projection image before reconstruction. Five computer-generated sections through the bud neck after reconstruction (Figure 6, B–F) demonstrate numerous structural details, including lipid droplets and other organelles, with remarkable clarity. Studies to identify the structures seen at this level of resolution are in progress.

In summary, X-ray tomography generates unique 3-D reconstructions of whole yeast without the need for chemical fixatives or contrast enhancement. Because the isotropic high-resolution data set is based on the tomographically reconstructed local X-ray absorption, the information in these reconstructions is quantifiable, and because the cells were rapidly frozen from the living state and remain fully hydrated, the information retains biological fidelity. For the specimens shown here, the total radiation dose for the entire tomographic data set was between 10^8 and 10^9 Gy, and separate radiation tests conducted on biological specimens show that application of a 10-fold greater radiation dosage resulted in no detectable structural damage of the specimen at the resolution of the X-ray microscope. Detailed discussions of radiation damage during X-ray imaging, including a theoretical model of radiolysis and radiation damage experiments (Schneider, 1998; Weiss *et al.,* 2000), indicate that it is theoretically possible to resolve frozen hydrated struc-

tures as small as 10 nm without inducing significant structural changes. Given the resolution presently achieved, there are many interesting structures that would benefit from X-ray tomographic imaging. Examples include the 30-nm fibers of packaged chromosomal DNA, structures that are quite fragile and easily damaged during processing for transmission electron microscopy (TEM), and macromolecular complexes such as polysomes. The ability to localize molecules using immunogold labeling with X-ray imaging (Meyer-Ilse *et al.,* 2001) also enables collection of high-resolution, 3-D, quantifiable molecular information from whole cells and, with the addition of a second label, protein-protein interactions.

At the present time identification of structures seen with X-ray tomography is complex. Some cellular structures are easily identified, such as the very dense lipid droplets and large vacuoles. Many other structures, however, will require more than direct comparison with TEM. Cryo-TEM generates extremely low contrast images, and cells examined using standard TEM techniques have typically been treated with chemicals (fixatives, contrast enhancement, and dehydrating reagents) that can alter structures and embedded in plastics that obscure structures. Images obtained using X-ray tomography are based on absorbance and the natural contrast of biological material. By measuring the X-ray absorption coefficient, very small differences in density are detected yielding complex images and increased structural details (for optimized measurements, <1% differences should be possible). To aid in identification, we are now systematically identifying structures seen in the yeast using the vast collection of green fluorescent protein fusions of proteins that serve as excellent markers for the organelles and microdo-

mains of yeast cells. This will provide a 3-D map of the structural organization of the yeast throughout the cell cycle. It is important to note that the achievable resolution with X-ray tomography continues to improve as do methods for nanofabrication of the optics and data collection. A completely automated cryo-tilt stage has just been completed that collects 180 images at 1° intervals, which will improve the resolution of the reconstructed data (Baumeister *et al.*, 1999) to ~35 nm, and future improvements in optics will bring it to sub–20-nm resolution. This, in addition to the fact that it only requires 3 min to image an entire cell, make it possible to conduct high-throughput analyses to determine the phenotypic consequences of genetic mutations and to obtain quantifiable information about the number and location of molecules in the entire cell.

ACKNOWLEDGMENTS

REFERENCES

Baumeister, W., Grimm, R., and Walz, J. (1999). Electron tomography of molecules and cells. Trends Cell Biol. *9*, 81–85.

Fernandez, J.J., Lawrence, A.F., Roca, J., Garcia, I., Ellisman, M.H., and Carazo, J.M. (2002). High-performance electron tomography of complex biological specimens. J. Struct. Biol. *138*, 6–20.

Frank, J., Radermacher, M., Penczek, P., Zhu, J., Li, Y.H., Ladjadj, M., and Leith, A. (1996). Spider and web—processing and visualization of images in 3d electron microscopy and related fields. J. Struct. Biol *116*, 190–199.

Gavin, A.C. *et al.* (2002). Functional organization of the yeast proteome by systematic analysis of protein complexes. Nature *415*, 141–147.

Grimm, R., Singh, H., Rachel, R., Typke, D., Zillig, W., and Baumeister, W. (1998). Electron tomography of ice-embedded prokaryotic cells. Biophys. J. *74*, 1031–1042.

Ho, Y. *et al.* (2002). Systematic identification of protein complexes in Saccharomyces cerevisiae by mass spectrometry. Nature *415*, 180–183.

Kumar, A. *et al.* (2002). Subcellular localization of the yeast proteome. Genes Dev. *16*, 707–719.

Kumar, A., and Snyder, M. (2002). Protein complexes take the bait. Nature *415*, 123–124.

Marsh, B.J., Mastronarde, D.N., Buttle, K.F., Howell, K.E., and McIntosh, J.R. (2001). Organellar relationships in the Golgi region of the pancreatic beta cell line, HIT-T15, visualized by high resolution electron tomography. Proc. Natl. Acad. Sci. USA *98*, 2399–2406.

Martone, M.E., Deerinck, T.J., Yamada, N., Bushong, E., and Ellisman, M.H. (2000). Correlated 3D light and electron microscopy: use of high voltage electron microscopy and electron tomography for imaging large biological structures. J. Histotechnol. *23*, 261–270.

Medalia, O., Weber, I., Frangakis, A.S., Nicastro, D., Gerisch, G., and Baumeister, W. (2002). Macromolecular architecture in eukaryotic cells visualized by cryoelectron tomography. Science *298*, 1209–1213.

Meyer-Ilse, W. *et al.* (2001). High resolution protein localization using soft X-ray microscopy. J. Microsc. *201*, 395–403.

Nicastro, D., Frangakis, A.S., Typke, D., and Baumeister, W. (2000). Cryo-electron tomography of Neurospora mitochondria. J. Struct. Biol. *129*, 48–56.

O'Toole, E.T., Winey, M., and McIntosh, J.R. (1999). High-voltage electron tomography of spindle pole bodies and early mitotic spindles in the yeast Saccharomyces cerevisiae. Mol. Biol. Cell *10*, 2017–2031.

Schneider, G. (1998). Cryo X-ray microscopy with high spatial resolution in amplitude and phase contrast. Ultramicroscopy *75*, 85–104.

Schneider, G., Anderson, E., Vogt, S., Knochel, C., Weiss, D., Legros, M., and Larabell, C. (2002). Computed tomography of cryogenic cells. Surf. Rev. Lett. *9*, 177–183.

Weiss, D., Schneider, G., Niemann, B., Guttmann, P., Rudolph, D., and Schmahl, G. (2000). Computed tomography of cryogenic biological specimens based on X-ray microscopic images. Ultramicroscopy *84*, 185–197.